Available online at www.sciencedirect.com

ScienceDirect

Advances in Space Research 56 (2015) 449–460

ADVANCES IN SPACE RESEARCH (a COSPAR publication)

www.elsevier.com/locate/asr

The Criticality of Spacecraft Index

A. Rossi [a,*], G.B. Valsecchi [a,b], E.M. Alessi [a]

[a] IFAC-CNR, Via Madonna del Piano 10, 50019 Sesto Fiorentino, Italy
[b] IAPS-INAF, via Fosso del Cavaliere 100, 00133 Roma, Italy

Received 27 October 2014; received in revised form 17 February 2015; accepted 22 February 2015
Available online 2 March 2015

Abstract

The future space debris environment will be governed by the production of fragments coming from massive breakups. In order to identify the most relevant parameters influencing the long term evolution of the environment and to assess the criticality of selected space objects in different regions of the circumterrestrial space, a large parametric study was performed. In this framework some indicators were produced to quantify and rank the relevance of selected fragmentations on the long term evolution of the space debris population. Based on the results of the fragmentation studies, a novel analytic index, the Criticality of Spacecraft Index (CSI), aimed at ranking the environmental criticality of abandoned objects in Low Earth Orbit (LEO), was formulated. It takes into account the physical characteristics of a given object, its orbit and the environment where this is located. The results corresponding to a sample of LEO objects in the initial population at the epoch of January 1, 2020 and mass larger than 100 kg are shown.

Keywords: Space debris; Fragmentations; Long term evolution; Space environment

1. Introduction

The simulations of the long term evolution of the space debris population, under realistic assumptions, show how the driving factor in the future environment will be mostly the breakup of large spacecraft and rocket bodies in LEO. A first warning in this respect came from the well known collision between Iridium 33 and Cosmos 2251 in 2009 which injected thousands of fragments larger than 1 cm into long lasting orbits in the most crowded zone of LEO, around 800–900 km of altitude. In this context, it is of paramount importance to understand the effects on the environment of a possible future large fragmentation of a given spacecraft in different regions of space.

The present distribution of intact objects is a good proxy to identify those more prone to future catastrophic collisions, by quantifying the collision risk and the associated consequences in the coming decades. This kind of analysis was performed by comparing the long term evolution of the space debris population when a given fragmentation occurs at a given epoch with the one when it does not happen. The reference scenario was defined by simulating space activities in a way analogous to the one adopted in the last decade. By evaluating the effects corresponding to the breakup of different masses moving on different orbits, it was possible to characterize *typical* fragmentation events and to distinguish the main parameters determining the criticality of a given abandoned space asset.

As a matter of fact, a quantitative measure of the criticality of the artificial objects in LEO would be important under different aspects. It would be a measure of the perspective danger posed to the environment in case an object would become non-cooperative, and therefore could be used to rank active removal priorities. Moreover, it would help spacecraft operators in easily assessing the present collision risk faced by a given asset in space, and thus driving

* Corresponding author.
E-mail addresses: a.rossi@ifac.cnr.it (A. Rossi), giovanni@iaps.inaf.it (G.B. Valsecchi), em.alessi@ifac.cnr.it (E.M. Alessi).

http://dx.doi.org/10.1016/j.asr.2015.02.027
0273-1177/

possible mitigation actions (e.g., disposal strategies). Moreover, as is the case of the Palermo Scale (Chesley et al., 2002) in the Near Earth Objects field, it could serve as a good mean to spread the public awareness of the danger posed by space debris by allowing a wider non-specialist audience to catch, with a single number, the environmental criticality of a given spacecraft.

Having these issues in mind, we present the Criticality of Spacecraft Index (hereafter, CSI), an analytical tool, easy and swift to compute, which grabs the importance of the parameters identified by simulating selected fragmentations. Despite of the name, the final goal is not to incriminate specific space objects, rather to measure the danger represented by *typical* classes of objects, in order to be able to rank the abandoned space objects in terms of the possible effects on the environment of the spacecraft and, conversely, in terms of the effect of the environment on the spacecraft itself.

2. Fragmentation ranking

Using SDM 4.2, the latest version of the long term LEO to GEO debris environment evolution model developed by our research group at the Italian National Research Council (CNR) in the past decades (Rossi et al., 2009), a reference long term evolution scenario was simulated for a time span of 200 years. With reference scenario, we mean that the traffic launch repeats an 8-year cycle representing the current launch pace, an 8-year lifetime is assumed for future spacecraft, no new explosions are considered and no avoidance maneuvers are performed. A post mission disposal scenario according to the 25-year rule is adopted, with a 60 % compliance to this rule. This compliance is computed based on the spacecraft that do not re-enter naturally in 25 years (i.e., only 60% of the spacecraft are actually de-orbited at end-of-life). On top of this reference scenario a number of different spacecraft were supposed to fragment in selected epochs. The different cases were simulated with 50 Monte Carlo runs and averages of the evolutions were computed. The above assumptions are common to most of the recent studies of the long term evolution of the space debris population. As in most of the modeling works, there are of course uncertainties related to these assumptions, e.g. the traffic launch cannot be predicted accurately for 200 years in the future, as well as the solar activity, etc. Nonetheless the above assumptions represent good, standard hypothesis that are well suited to produce an "average" reliable future environment appropriate for the purpose of the present study. Comparing the long term evolution in the cases with and without the additional fragments generated by the artificially introduced fragmentation, the effect of the particular fragmentation on the environment was evaluated.

This study was conducted in the framework of the ESA-ESOC Contract "*Assessment Study for Fragmentation Consequence Analysis for LEO and GEO Orbits*". The full results are under final review and cannot be shown here. In this paper, we intend to present the analysis methods envisaged for this study, along with a few sample results.

Fig. 1 shows the number of objects larger than 10 cm in LEO produced in the reference case (thick blue line), averaged over 50 Monte Carlo runs. Note that 50 runs might be on the lower limit for a robust statistics (e.g., to compute higher order moments of the distribution) (Liou, 2008) but it has been shown in many previous papers (and also within the IADC comparison works) that this number still provides meaningful evolutions. The thin blue lines in Fig. 1 represent the $\pm 1\sigma$ standard deviation of the Monte Carlo simulations. The other three curves represent the number of objects obtained in scenarios where the fragmentation of a spacecraft resembling the Envisat polar platform (mass $\simeq$ 8000 kg) is artificially introduced in the simulation. In particular, it was assumed that this additional fragmentation would take place in the year 2020 (red line) or in year 2070 (magenta line) or in year 2095 (black line). The Envisat fragmentation is supposed to take place in a decaying orbit, i.e., the same spacecraft is always fragmented but at different altitudes according to the epoch, from about 760 km of altitude in the year 2020 to about 695 km in 2095.

Contrary to what one might expect, the final number of objects in all the four cases is statistically the same (i.e., all well within the $\pm 1\sigma$ standard deviation bounds). From a statistical point of view, the Envisat fragmentations shown in Fig. 1 are leading to a long term LEO environment which is indistinguishable from the reference one. This means that, *in the long run*, even the fragmentation of a very large spacecraft leaves no noticeable signature on the environment or, in other words, the simulated Envisat fragmentation does not alter, by itself, "permanently" the LEO environment on the long run (200 years). The reason for this outcome is that the reference evolution is highly stochastic and is dominated by a large number of fragmentations (on average one every 5 years). Therefore, the effects of our additional Envisat-like fragmentation get soon "diluted" in the vast number of background fragments and leave almost no trace after 200 years. On the other hand, the situation can be different in the "interim" regime, in the orbital regions in the vicinity of the Envisat fragmentation, during the few decades following the event; these shorter term effects have been studied too and will be described elsewhere. The small jump in the reference curve around the year 2115 is due to a chance accumulation of large fragmentations happening around that epoch in a few MC runs. Even if this discontinuity would be better levelled out if many more MC runs would be performed, it was checked that the long term evolution used as reference is reliable and well consistent, also by comparing with the results of the same scenario obtained with other independent long term evolution codes (Rossi et al., 4000).

In order to analyze many different long term evolution scenarios, it is necessary to find an evaluation norm to order the events in terms of their danger for the environment. For this purpose we devised a norm able to quantify

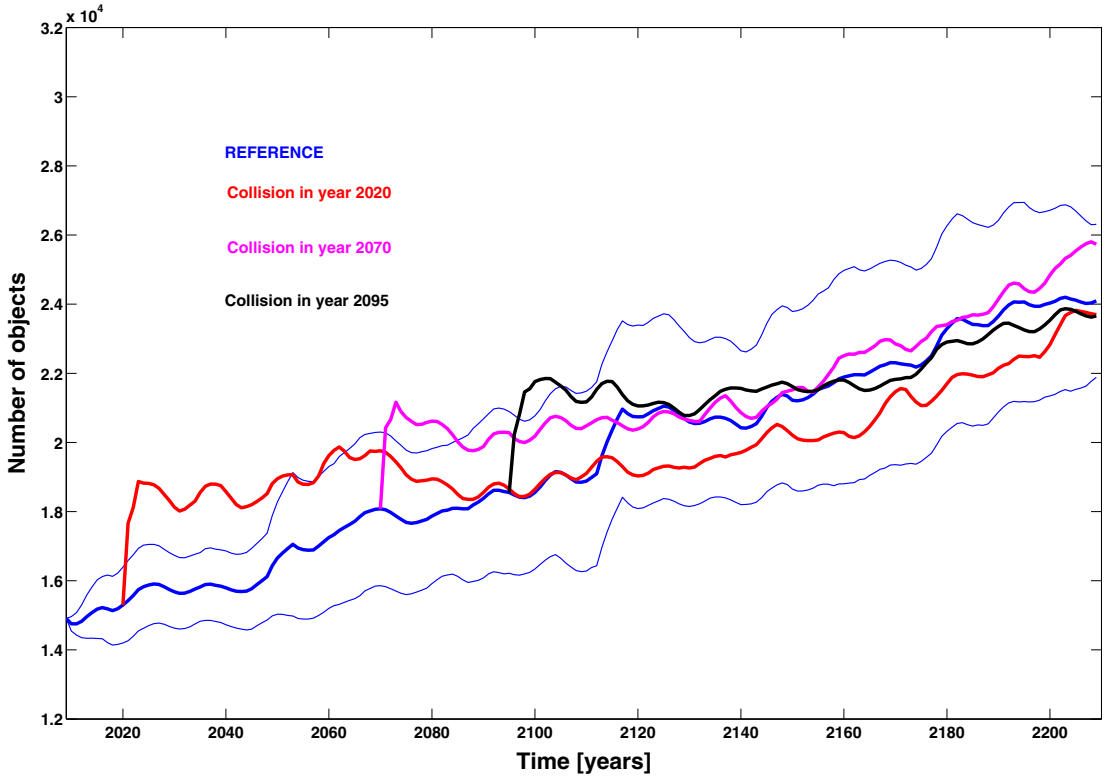

Fig. 1. Number of objects larger than 10 cm in the reference scenario (blue line) and in 3 cases where a fragmentation of Envisat happens at three different epochs: 2020 (red line), 2070 (magenta line) and 2095 (black line). The thin blue lines represent the $\pm 1\sigma$ standard deviation of the reference case. (For interpretation of the references to color in this figure legend, the reader is referred to the web version of this article.)

and easily visualize these results. Given an underlying reference scenario and a fragmentation scenario in which the simulation of a particular fragmentation is added, the growth of the population of the fragmentation scenario with respect to the reference one can be quantified by:

$$C_i = \left(\frac{n_{FRAG}(i) - n_{REF}(i)}{\sigma_{REF}(i)} \right), \tag{1}$$

if $(n_{FRAG}(i) - n_{REF}(i)) \geqslant 0$ else $C_i = 0$; n_{FRAG}, n_{REF} and $\sigma_{REF}(i)$ represent, for the ith year, the number of objects in the fragmentation case, the number of objects in the reference case and the standard deviation of the reference Monte Carlo runs, respectively.

As an example, Fig. 2 plots the value of C_i in the case of the Envisat fragmentation scenarios shown in Fig. 1. The decreasing relative importance of the fragmentations happening in later years (both due to the larger number of background fragments and, mainly, to the lower altitude of the event) is clearly highlighted here.

A ranking of the danger represented by selected fragmentations can be easily expressed with a single number. In fact, the sum of the differences, weighted by the time interval, gives an indication of the criticality:

$$C^* = \sum_{i=1}^{N} \frac{C_i}{N} = \sum_{i=1}^{N} \left(\frac{n_{FRAG}(i) - n_{REF}(i)}{\sigma_{REF}(i)} \right) \Big/ N, \tag{2}$$

if $(n_{FRAG}(i) - n_{REF}(i)) \geqslant 0$ else $C_i = 0$; N is the number of years in the simulation. In the ESA study a full ranking of a large number of different fragmentations is being elaborated and will be soon published in a forthcoming paper.

Based on the considerations and conclusions obtained from the analysis of the wealth of data produced by simulating different fragmentations in various orbital regimes, a way to classify space objects in LEO was devised. This classification criterium is the subject of the next Section.

3. The Criticality of Spacecraft Index

We start by noting that the CSI applies in principle to abandoned objects (debris) since an active object, able to perform avoidance maneuvers, could theoretically avoid most of the collisions with debris larger than 10 cm if an efficient Space Surveillance network is in place. Moreover, the CSI is useful only for large objects; in fact, small, centimeter sized objects, although possibly very dangerous as projectiles, do not represent a threat to the environment at large if fragmented, since they would not generate large debris clouds.

Given the expected usage of such an index, it should take into account the characteristics of the environment where the object moves, as well as the physical and orbital details of the objects itself. In our case the environment is

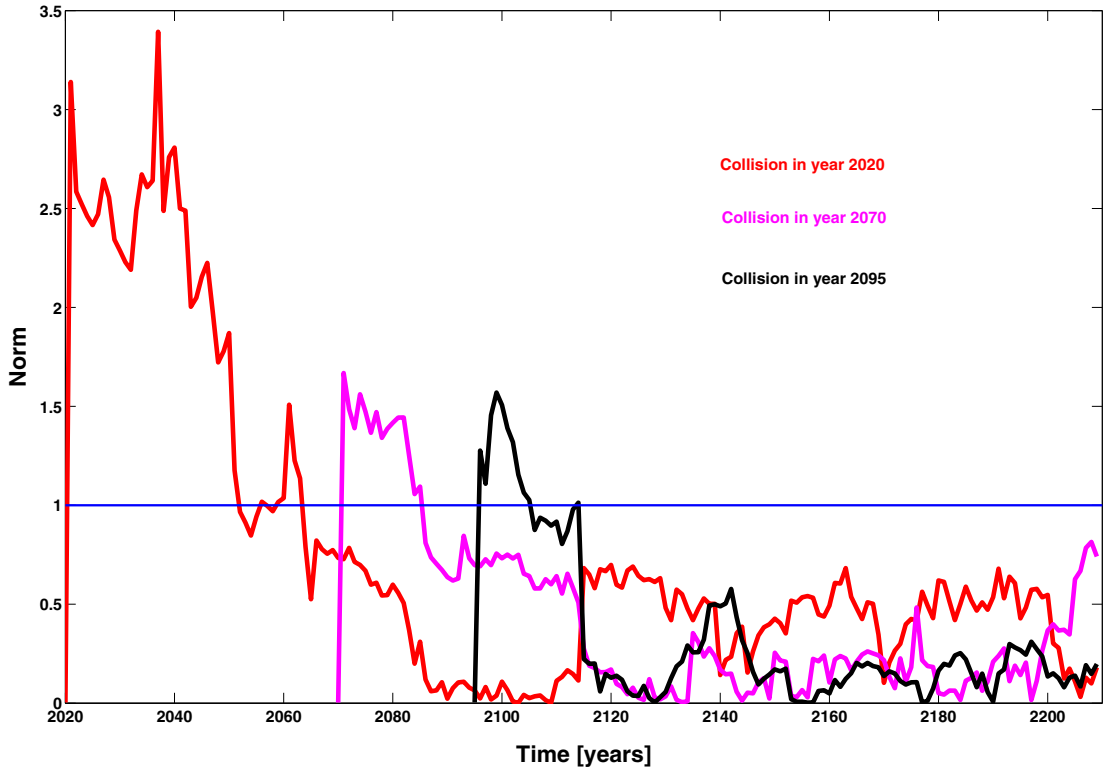

Fig. 2. The time evolution of the norm of Eq. (1), computed for the three Envisat-like fragmentations, shown in Fig. 1.

considered in terms of the spatial density of objects, together with the residual lifetime in space, the mass and the inclination of the orbit. In the following subsections each one of these dependencies is discussed and detailed. Moreover, the CSI can be computed either for a specific epoch or as an average for a given interval of time.

3.1. Environment dependence

The environment is considered in terms of the spatial density of objects as a function of time and altitude. It is well known that the collision probability is higher in regions where a higher concentration of objects is found. For this purpose, a simulation of the evolution of the space debris environment, spanning 200 years (considering the population of objects larger than 10 cm from the MASTER 2009 population), was performed with SDM 4.2 (Rossi et al., 2009). The reference scenario as the one described in the previous section was adopted to this end. The resulting spatial density of objects as a function of altitude was recorded every year and stored. As an example, Fig. 3 shows the spatial density of objects larger than 10 cm as a function of altitude, for three different epochs.

The way in which the spatial density is taken into account in the CSI is as follows: given an epoch (or interval of time) and the orbital altitude, h, of the object under consideration, the spatial density, D, is taken from the stored values and normalized to the value of the maximal spatial density in the initial year 2009, that is the one at the altitude of 770 km, D_0. Therefore, the multiplicative contribution to the CSI accounting for the environment density is given by:

$$\frac{D(h)}{D_0}.$$

3.2. Lifetime dependence

The danger represented by an object left in space and the probability that it will be destroyed by a collision is a function of the time that this object will spend in space. Moreover the long term consequences of a fragmentation are much more severe for events happening at high altitudes where the cleaning effects of the atmosphere are not effective. Therefore the residual lifetime of an object is an important parameter to include in the index computation.

The lifetime for the objects, as a function of the orbital altitude h, is estimated from an average lifetime given by the curve shown in Fig. 4. The lifetimes points were kindly computed by Anselmo and Pardini using the code SATRAP (Pardini and Anselmo, 1994), assuming an area over mass ratio, $A/M = 0.012\ \mathrm{m^2\ kg^{-1}}$ which reflects the average value observed for intact objects (since, as mentioned above the index is thought to be applied to large abandoned objects), and an average solar flux between 110 and 130 units. The lifetime curve was computed as power law fit of the form:

$$\log(life) = ah^b + c, \tag{3}$$

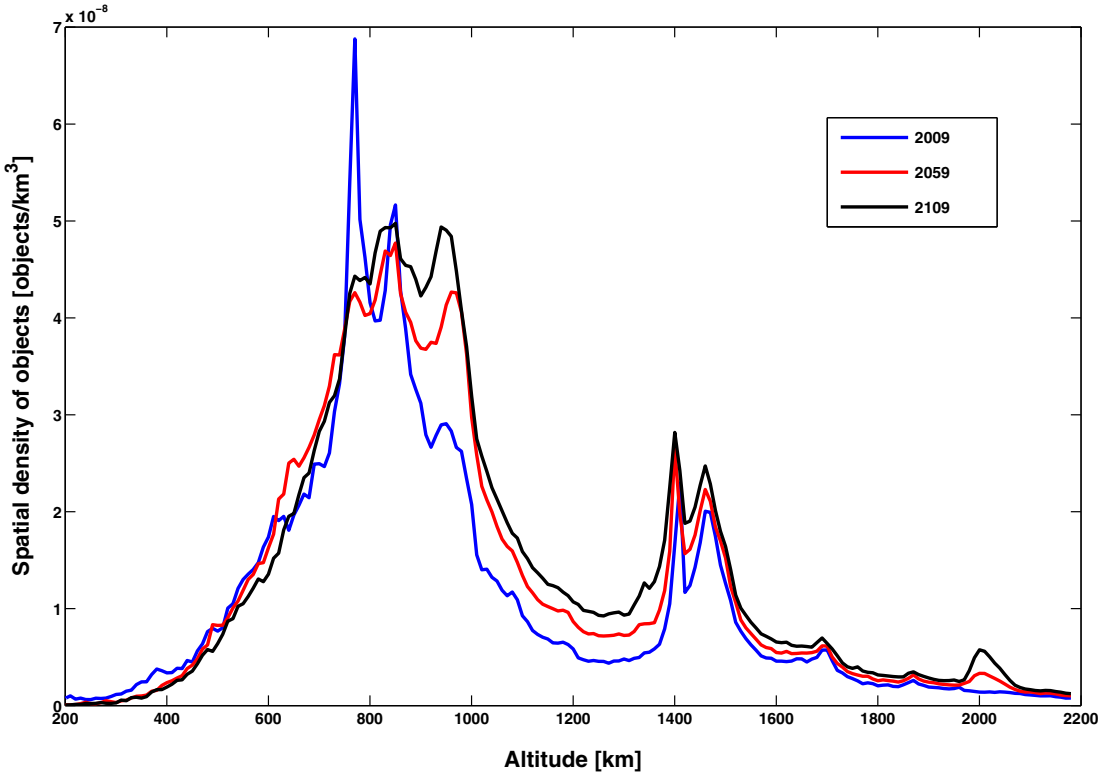

Fig. 3. Spatial density of objects as a function of altitude in three different epochs: 2009 (blue line), 2059 (red line) and 2109 (black line). The densities are derived from the simulations performed with SDM on the Reference scenario described in detail in the text. (For interpretation of the references to color in this figure legend, the reader is referred to the web version of this article.)

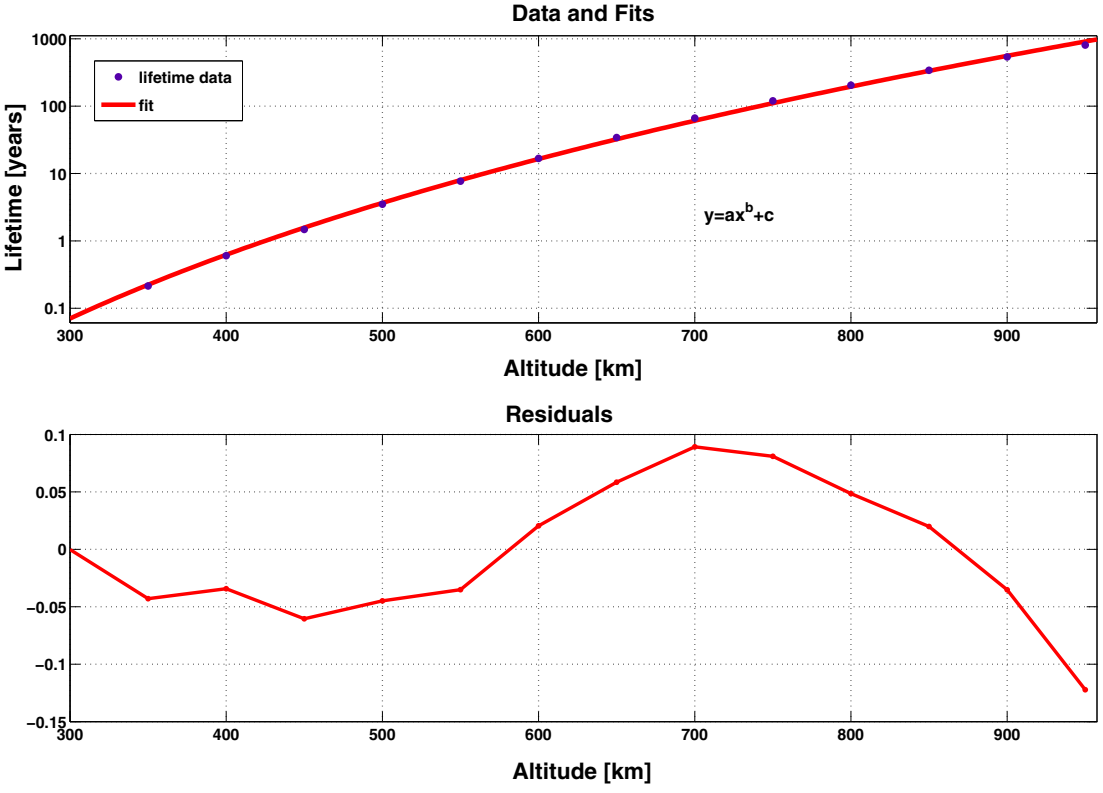

Fig. 4. Orbital lifetime of a sample object with $A/M = 0.012\ \mathrm{m^2\ kg^{-1}}$ as a function of altitude. The upper panel shows a power law fit to the lifetime values and the bottom panel shows the residuals of the fit (see text for details).

where $a = 14.18$, $b = 0.1831$ and $c = -42.94$ are the coefficients of the fit. Therefore, given an object with mean altitude h (note that, for LEO objects having low eccentricity, the semimajor axis can be used as a good approximation of h), the CSI component accounting for the lifetime is given by:

$$\frac{life(h)}{life(h_0)},$$

where $life(h)$ is computed with Eq. (3) and the normalizing value is computed, as a default, for $h_0 = 1000$ km.

3.3. Mass dependence

Along with the altitude of the event, the other most influential parameter in determining the environment consequences of a given fragmentation is the mass, M. This is taken into account in the CSI by including the term:

$$\frac{M}{M_0},$$

where the normalizing factor is arbitrarily taken as $M_0 = 10,000$ kg. An alternative that we explored is to use the same exponent found in the NASA breakup model by putting the mass terms to:

$$\left(\frac{M}{M_0}\right)^{0.75}.$$

It has been checked that the adoption of the 0.75 exponent does not change significantly the results. Therefore, for the sake of simplicity, in the following the value of the exponent used is 1.

3.4. Inclination dependence

It is well known that the collision risk is maximum for high inclination orbits that can cross all the other orbits in their range of altitude and that can lead to very high mutual inclinations (and therefore high impact velocities) due to the precessing orbital planes. For this reason an inclination, i, dependence is included in the CSI, in the form:

$$\frac{1 + k\,\Gamma(i)}{1 + k},$$

where:

$$\Gamma = \frac{1 - \cos(i)}{2},$$

and $k = 0.6$ since the typical flux of debris on an almost equatorial orbit is about 60% of the flux on a polar orbit. Note that the Γ expression is devised in order to properly weight retrograde orbits, which would be underweighted if a simple $\sin(i)$ term would be included.

3.5. Index definition

Combining the terms described above, the final definition of the CSI, denoted with Ξ, reads as:

$$\Xi = \frac{M(h)}{M_0}\,\frac{D(h)}{D_0}\,\frac{life(h)}{life(h_0)}\,\frac{1 + k\,\Gamma(i)}{1 + k}. \tag{4}$$

The definition was kept as simple as possible in order to allow its easy application and understanding by the largest possible community; the larger the value of the CSI, the more dangerous to the environment is *an abandoned object.*

Note that, thanks to the normalization, for all the space objects in our population $\Xi < 1$. Note also that, in theory, it is not mathematically bound by 1 since, e.g., a hypothetical polar object exceeding 10 tons and orbiting around 1000 km of altitude could have $\Xi > 1$. In order to consider possible time variations in the environment, the CSI could also be computed taking into account the average density of objects over an interval of time (e.g., 10 years) instead of the single value in the year of reference.

4. An illustrative application

The CSI corresponding to the year 2020 was computed for every LEO object with mass larger than 100 kg listed in the MASTER 2009 population. Table 1 lists the first 15 objects having the largest values of the CSI in our population.

It is worth stressing that, at this stage, the purpose of the current study is not to compile a ranking of cataloged objects, pointing out which one is the most dangerous; rather, our goal here is to describe the CSI and show its potential applications. Therefore in our rankings presented below we will not list names of objects, but only physical and orbital characteristics. This will allow to identify families of objects particularly dangerous for the environment and prone to perspective active debris missions. As the only notable exception, we identify the top object in Table 1 as a *Zenit 2* upper stage, due to its distinct characteristic well known to the professionals in the field.

As it can be noticed, all the objects have large mass, well above one metric ton. However, it is also worth noting that

Table 1
List of the 15 objects having the largest values of the CSI in our MASTER 2009 population. Objects in boldface are upper stages, the others are satellites.

	a [km]	ecc	Inc. [deg]	Mass [kg]	Ξ
1	7372.2	0.002	99.25	9000.0	**0.313**
2	7365.7	0.003	64.98	4500.0	0.163
3	7343.1	0.003	64.99	4955.0	0.161
4	7342.1	0.004	65.04	4955.0	0.160
5	7355.2	0.006	64.49	4500.0	0.154
6	7346.5	0.007	65.28	4500.0	0.151
7	7342.9	0.006	64.95	4500.0	0.146
8	7349.3	0.005	64.81	4500.0	0.145
9	7332.1	0.005	64.98	4955.0	0.143
10	7222.0	0.001	71.00	9000.0	**0.139**
11	7221.6	0.000	70.98	9000.0	**0.139**
12	7336.6	0.004	64.70	4500.0	0.135
13	7227.3	0.002	70.88	8226.0	**0.135**
14	7335.5	0.006	64.86	4500.0	0.134
15	7333.3	0.009	65.08	4500.0	0.131

the ranking is not just dominated by the mass, given that the semimajor axis (i.e., the mean altitude) plays a significant role, and that all the objects in the table have high inclinations.

Figs. 5–10 graphically show the distribution of the CSI values, Ξ, as a function of different orbital and physical parameters for the highest 100 values obtained. In all the figures it can be noticed how all the highest index colors pertain to large objects, above a few metric tons. Moreover, all the top CSI values have perigee above about 600 km of altitude. The situation is less marked for the inclination distribution. Most of the massive objects have inclination larger than 50 degrees and, within this sample of large spacecraft, again the top CSI values pertain to high inclination orbits, as expected.

In Figs. 8–10 the objects appear as circles with diameters proportional to their mass. It is worth noting how the orbital distributions obtained compare nicely with Fig. 13 of Liou (2011), where the orbital distribution of the existing LEO R/Bs and S/Cs having highest mass and collision probability products (computed with 100 Monte Carlo runs of LEGEND) is shown. In particular, we can single out the following families:

- Soviet/Russian Cosmos satellites between 900 and 1000 km at an inclination of about $i \sim 65°$;
- SL-16 rocket bodies and Soviet/Russian Cosmos satellites around 850 km and $i \sim 72°$;
- SL-16 rocket bodies and Meteor satellites between 950 and 1000 km and $i \sim 83°$;
- rocket bodies and spacecraft in Sun Synchronous orbits between 750 and 1100 km and $95° \leqslant i \leqslant 100°$.

This is a further confirmation that the CSI can be considered as a reliable indicator of the actual risk faced and posed by objects in LEO and as such is a good analytic, fast and easy-to-compute proxy for active removal strategies planning.

Moreover, it is interesting to note that Fig. 10 points out that the majority of the top 100 values of CSI is composed by satellites, rather than by rocket bodies.

The histograms in Fig. 11 represent the distribution in altitude and inclination, respectively, of all the fragmentations recorded in the 50 Monte Carlo runs performed with SDM to derive the spatial density distributions, shown in Fig. 3 and used to compute the environment dependence as described in Section 3.1. They highlight the most dangerous zones in LEO in terms of the catastrophic collision risk. Within these histograms the red dots show the orbital parameters of the top 500 objects in the CSI ranking. It can be noticed how these objects clearly populate the bins where the highest number of collisions occur, once again showing that the CSI is an effective mean for the collision risk faced by a spacecraft in LEO.

5. State of the art and discussion

Recently, there have been other attempts to establish an indicator to rate the danger represented by a space asset. We give here a brief description of them, noting that in

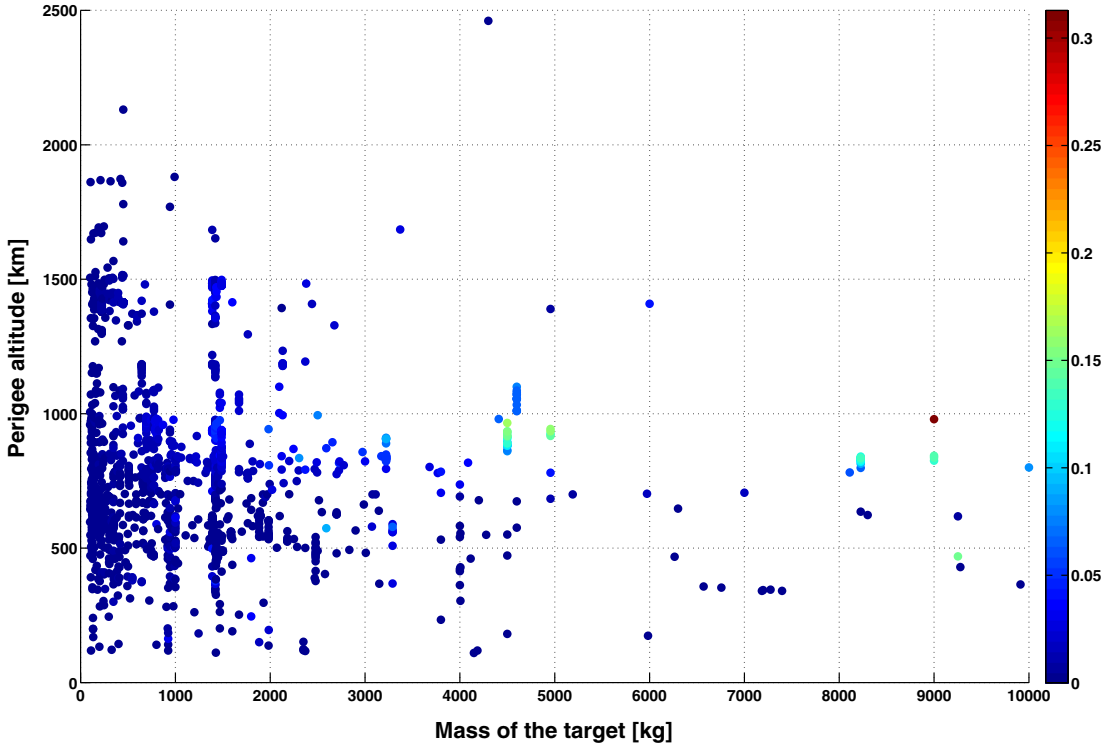

Fig. 5. The highest 100 values of Ξ in the perigee altitude vs. mass plane; the color of the points is coded according to the value of Ξ, as shown by the color bar. (For interpretation of the references to color in this figure legend, the reader is referred to the web version of this article.)

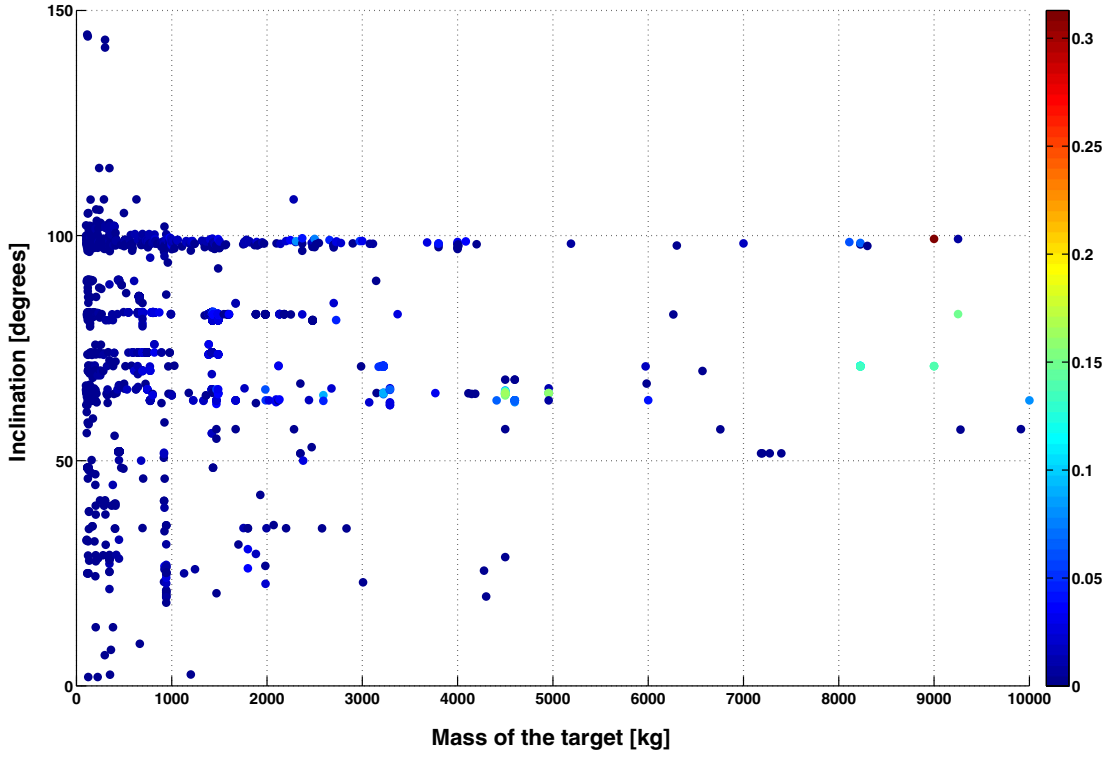

Fig. 6. The highest 100 values of Ξ in the inclination vs. mass plane; the color of the points is coded according to the value of Ξ, as shown by the color bar. (For interpretation of the references to color in this figure legend, the reader is referred to the web version of this article.)

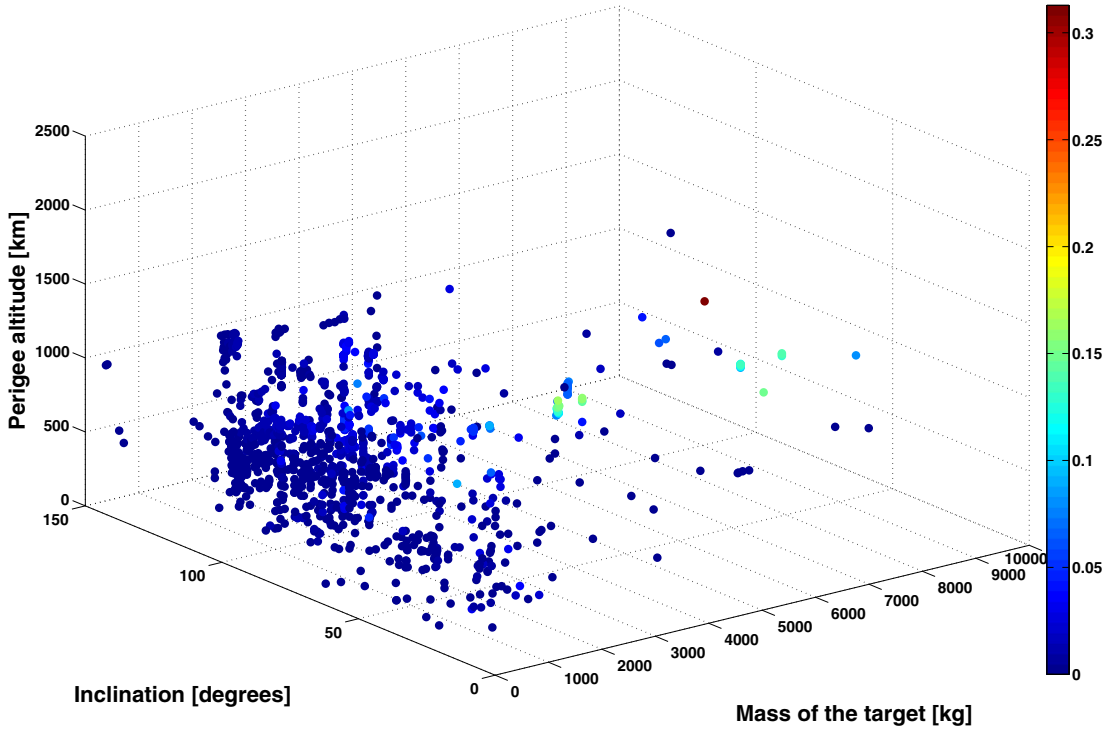

Fig. 7. The highest 100 values of Ξ in the space of perigee altitude, inclination and mass; the color of the points is coded according to the value of Ξ, as shown by the color bar. (For interpretation of the references to color in this figure legend, the reader is referred to the web version of this article.)

all the cases (ours included) the main vulnerability at the moment consists in the fact that the statistical nature of the evolution of the population is not taken into account.

Yasaka (2011) stressed the importance of providing a simple expression to represent the capability of a given orbiting object to yield debris fragments. He is aware that

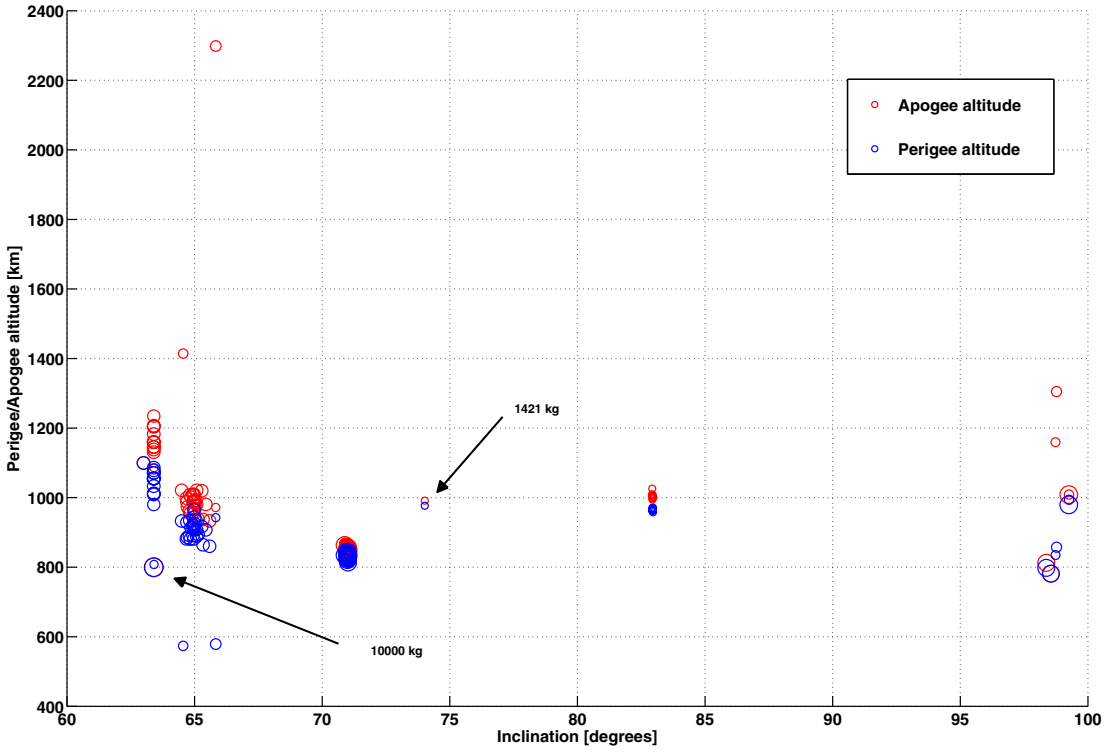

Fig. 8. Distribution of the first 100 objects in the Ξ ranking as a function of inclination and perigee (blue circles) and apogee (red circles). Note that each object is represented by two circles, one blue, for the perigee, and one red, for the apogee. The size of the circles is proportional to the mass of the object. (For interpretation of the references to color in this figure legend, the reader is referred to the web version of this article.)

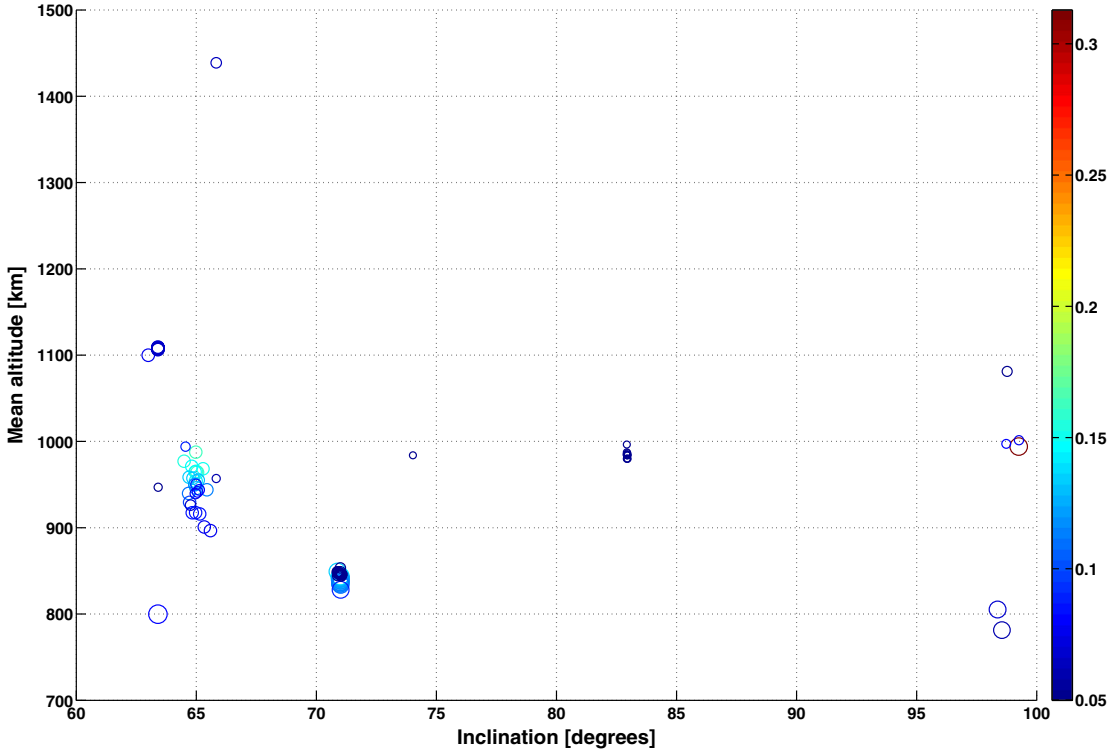

Fig. 9. Distribution of the first 100 objects in the Ξ ranking as a function of inclination and mean altitude. The color of the circles gives the value of the index, according to the color bar on the right, and the size of the circles is proportional to the mass of the object. (For interpretation of the references to color in this figure legend, the reader is referred to the web version of this article.)

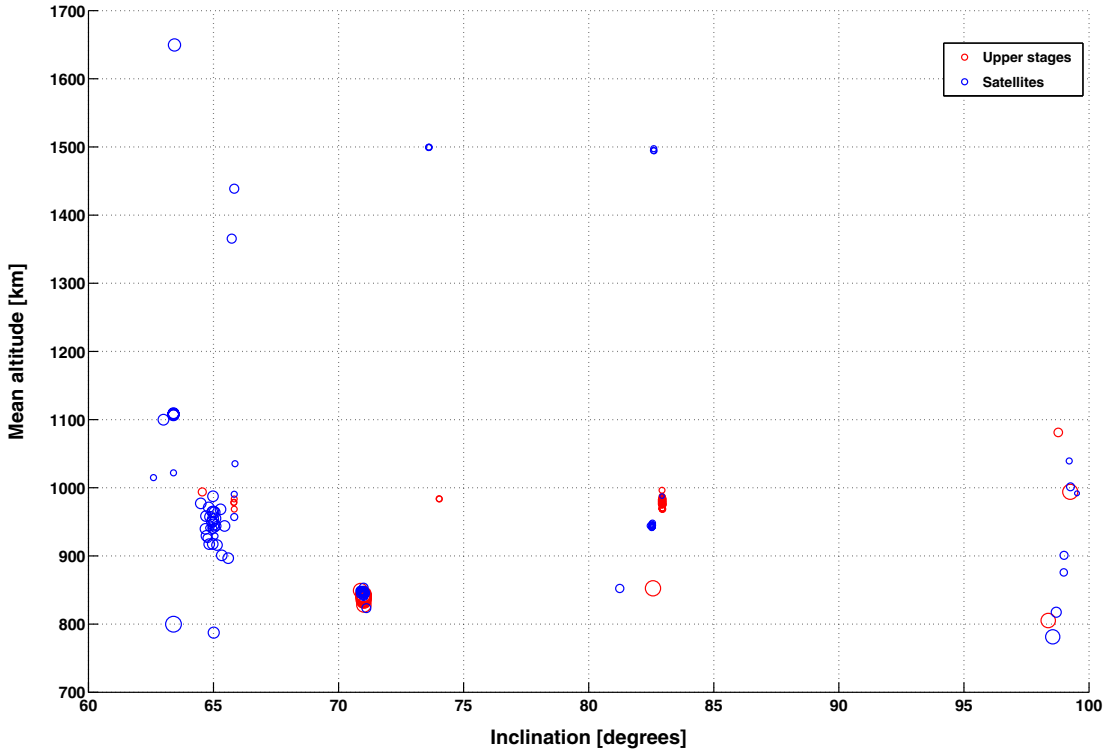

Fig. 10. Distribution of the first 100 objects in the Ξ ranking as a function of inclination and mean altitude. The blue circles relates to satellites while the red ones relate to upper stages. The size of the circles is proportional to the mass of the object. (For interpretation of the references to color in this figure legend, the reader is referred to the web version of this article.)

the resulting number will drive space system design, active debris removal priorities and also the public understanding of the issue. The formula he developed can, in principle, be applied to a body of any size, not necessarily non-operative, and in any orbit from LEO to GEO. From his point of view, the relevant parameters are the mass, the cross sectional area, and the lifetime of the object, together with the flux at a given altitude and a constant, α, giving the number of fragments that would be generated by the breakup of a given mass. The main drawback of his development is that the practical usage of his expression would require, as he also stated, detailed studies to obtain realistic values for α. Moreover, it is not clear how he estimates the orbital life of a body beyond the LEO region.

Utzmann et al. (2012) are motivated by the need of ranking active debris removal potential targets, and defining the corresponding mission profiles. The formula they gave applies to large LEO debris, and takes into account the mass (to the power 0.75 as in the NASA breakup model), the cross sectional area, the lifetime of the body and the flux corresponding to the orbit considered. The latter is taken from MASTER 2009, while the lifetime is computed by means of an Astrium internal software, not released to the public, as far as we know. The results they provide for the top 100 objects in their ranking resemble closely the ones shown in Fig. 8.

A more elaborate approach was considered by Lewis et al. (2013), who focused on a broader perspective in terms of "health" of the LEO environment. Contrary to the other tools presented here, given an object a higher score means than this object is more beneficial for the current space environment. Apart from mass, perigee altitude and inclination of the object, other features enter into their analysis, with an emphasis on the compliance of the current mitigation measures. The number of fragments generated in case of breakup is computed by means of the NASA model, though this is not the primary goal of their implementation, since the number of fragments is only one of the aspects considered to evaluate the environment impact rating of a given spacecraft.

Finally, Kebschull et al. (2014) introduced the 'Environment Criticality' index, defined as the product of a parameter representing the risk the LEO object is subject to times a parameter accounting for the impact of its fragmentation onto the space environment. They considered the contribution due to the cross sectional area of the orbiting body, the time from the fragmentation event, the time span covered by the simulation, and the flux. We understand that this estimate is closer to the norm introduced in Section 2 than to the CSI. In particular, their main effort was addressed to the development of a fast analytical tool to simulate the long term evolution of the environment.

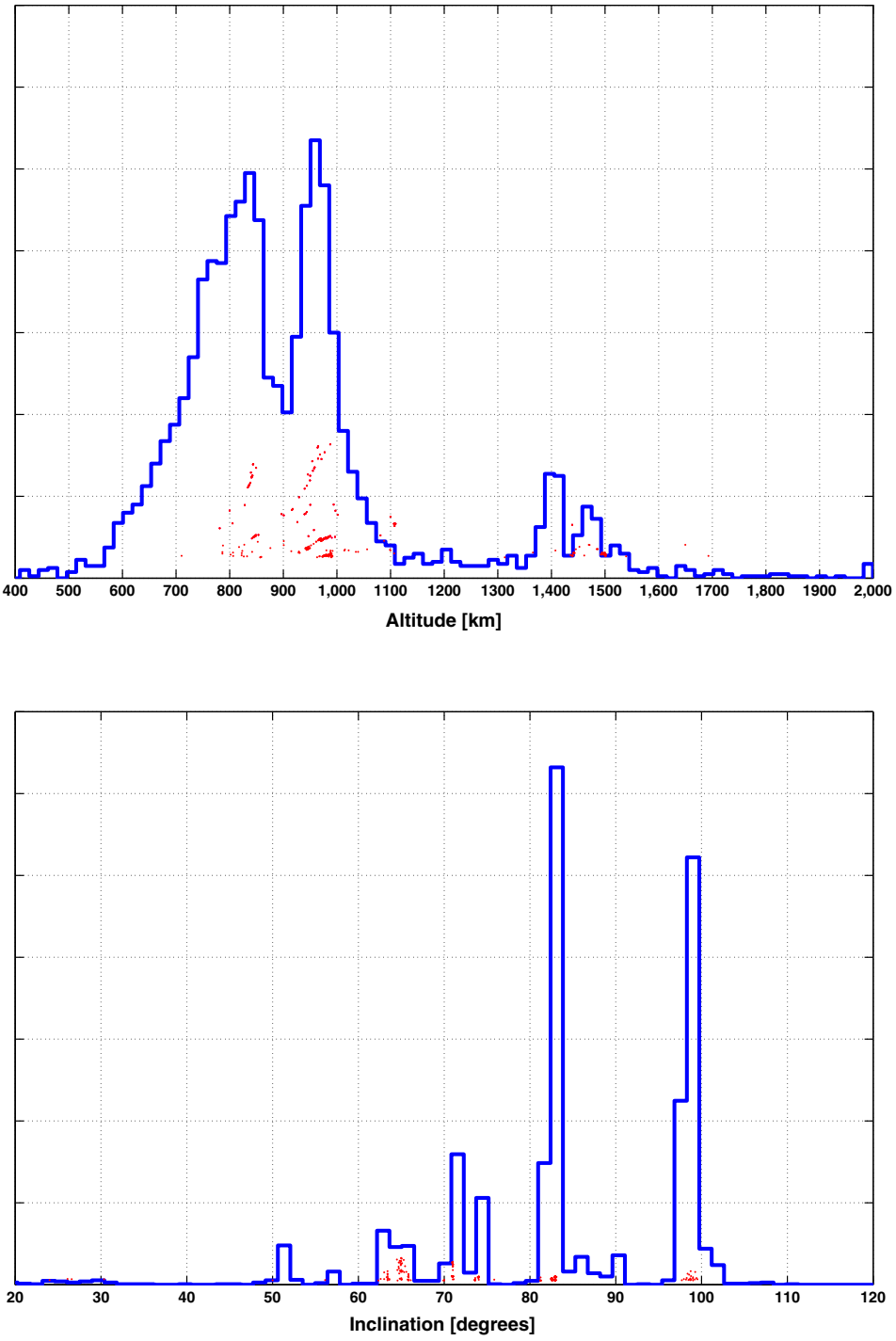

Fig. 11. Altitude (top panel) and inclination (bottom panel) relative distribution of all the fragmentations recorded, in the investigated 200-year time span, in all the Monte Carlo runs of the reference case used to derive the objects spatial density with SDM. The red dots show the altitude and inclination distribution of the first 500 objects in the CSI ranking. (For interpretation of the references to color in this figure legend, the reader is referred to the web version of this article.)

6. Conclusions and future work

The CSI index presented in the paper is a simple, fast, easy-to-compute analytic tool able to rank the abandoned space objects in term of the danger they can pose to the environment (or, conversely, in terms of the risk they face from the environment) taking into account their orbital and physical characteristics. It has been shown how it is able to catch the main known features of the in-orbit collision risk and that it can be viewed as a good proxy for active debris removal planning.

Further analysis and testing is under way. For instance, SDM 4.2 can simulate complex scenarios where active debris removal is used as a mean to stabilize the future environment. The parameter currently used in SDM 4.2 to decide which objects shall be removed in a given year is the standard parameter (*Mass* × *collision probability*). The validity of the CSI as a prioritization ranking for active debris removal targets will be further tested by implementing it in SDM 4.2, and the long term evolutions of the environment obtained using the CSI and those obtained using the standard parameter will be compared.

Moreover, the possibility to directly couple the C^* norm results within the CSI, to even better evaluate the consequences of future single fragmentations is under evaluation.

Finally a way to incorporate long term evolution uncertainties – both "formal uncertainties" from the Monte Carlo averaging and "systematic" modeling uncertainties (i.e., upper and lower ranges of evolutions due to parameters choice in the physical models such as solar flux, atmospheric density, fragmentation threshold, ...) – into the index computations (e.g., in the yearly density terms) are being explored.

Acknowledgments

The study described in the paper was performed in the framework of the contracts: *SPARC-Space Threats and Critical Infrastructures: Risks and Countermeasures (HOME/2011/CIPS/AG/4000002119)* and *Assessment Study for Fragmentation Consequence Analysis for LEO and GEO Orbits*, ESA/ESOC No. 4000106534/12/F/MOS. Part of this research was performed in the framework of the FP7-PEOPLE-2012-ITN *Stardust- The Asteroid and Space Debris Network*. The authors wish to thank the anonymous reviewers for their very careful comments that helped to improve the paper.

References

Chesley, S.R., Chodas, P.W., Milani, A., Valsecchi, G.B., Yeomans, D.K., 2002. Quantifying the risk posed by potential Earth impacts. Icarus 159, 423–432.

Kebschull, C., Radtke, J., Krag, H., 2014. Deriving a priority list based on the environmental criticality, paper IAC-14-A6,P,48,x26173. In: 65th International Astronautical Congress, Toron to, Canada.

Lewis, H., George, S., Schwarz, B., Stokes H., 2013. Space debris environment impact rating system. In: Proceedings of the Sixth European Conference on Space Debris, ESA SP-723, CD-ROM, ESA Communication Production Office, Noordwijk, The Netherlands.

Liou, J.-C., 2008. A statistical analysis of the future debris environment. Acta Astronaut. 62 (2), 264–271.

Liou, J.-C., 2011. An active debris removal parametric study for LEO environment remediation. Adv. Space Res. 47, 1865–1876.

Pardini, C., Anselmo, L., 1994. SATRAP: satellite reentry analysis program. Internal Report C94-17, CNUCE/CNR, Pisa, Italy, 30 August 1994.

Rossi, A., Anselmo, L., Pardini, C., Jehn, R., Valsecchi G.B., The new Space Debris Mitigation (SDM 4.0) long term evolution code, in: Proceedings of the Fifth European Conference on Space Debris, ESA SP-672, CD-ROM, ESA Communication Production Office, Noordwijk, The Netherlands, 2009.

Rossi, A., Lewis, H., 2015. The long-term environment evolution results, Version 1.0. Study Note for the Contract Assessment Study for Fragmentation Consequence Analysis for LEO and GEO Orbits, ESA/ESOC No. 4000106534/12/F/MOS, January 2015.

Utzmann, J., Oswald, M., Stabroth, S., Voigt, P., Wagner, A., Retat, I., 2012. Ranking and characterization of heavy debris for active debris removal, paper IAC-12-A6,2,8,x14182. In: 63rd I nternational Astronautical Congress, Naples, Italy.

Yasaka, T., 2011. Can we have an end to the debris issue? paper IAC-11-A6,5,1. In: 62nd International Astronautical Congress, Cape Town, South Africa.